

Radial Stiffness of Combined Journal and Thrust Hydrostatic Bearing

Małgorzata SIKORA

*Institute of Machine Tools and Production Engineering
Lodz University of Technology
Stefanowskiego 1/15, 90-924 Łódź, Poland
norbertkepczak@dokt.p.lodz.pl
witold.pawlowski@p.lodz.pl*

Received (20 June 2016)

Revised (26 July 2016)

Accepted (18 August 2016)

The paper presents the results of theoretical analysis of the effect of supply pressure and rotational speed on the radial stiffness of the integrated angular cylindrical-face hydrostatic bearings designed for precise technological devices. The obtained theoretical results were verified experimentally using the spindle system of the grinding wheel of cylindrical grinder.

Keywords: hydrostatic bearing, combined journal, integrated angular, stiffness.

1. Introduction

The continuous search for a more perfect way of the realization of rotational or advance motion of assemblies of technological devices has determined the development of technology of hydrostatic lubrication. This is particularly important in the machine tool industry, where the machining accuracy depends on the spindle unit. The advantages such as high accuracy of motion, high load capacity and rigidity, damping of vibration and a very low frictional resistance even at start-up, resulted in that the hydrostatic bearings are currently used in machine tools, in such cases, where other varieties of bearings can not meet the extreme requirements [1]. They are indispensable when demands are toward particularly high precision spindle running and excellent vibration damping. Compared with the hydrodynamic and rolling bearings they allow for repeated reduction in run out of the spindle [2–4] as well as the obtaining the mirror smoothness of the machined surface [5]. They are suitable for very heavy static and dynamic loads. Additionally, they have a high stiffness in the range of low loads, typical for the operating conditions of precision machine tools. These bearings can operate at very low (including zero) and very high rotational speeds. In a properly designed and operated hydrostatic bearing it

never comes to the metallic contact of journal and sleeve during operation, which provides practically unlimited service life (durability) of such bearings.

In general, to support the machine spindle with hydrostatic bearings there are required two radial bearings and one two-sided axial (thrust) bearing. Sometimes the integrated (combined) radial-axial bearings, which are adapted to simultaneously, transfer of radial and axial forces. The application of such bearings allows simplifying the design of the spindle unit. Power losses in these bearings are smaller than in the independent axial and radial bearings. In addition, the integrated bearings (combined) enable a reduction in oil flow, which reduces the output of pump supplied the system. The result is a simpler design, easier to make, cheaper and more favourable in terms of energy [6-9].

Among the hydrostatic axial-radial bearings it is distinguished cylindrical-face bearing (Fig. 1), which is described in the literature for a long time - the most detailed in the books that can be considered as a classic in this field [7-9]. Rowe called them Yates bearings. Although neither mentioned books nor the present time books or manuals [10-13] does not take into account adequately an effect of rotational speed on the properties of these bearings, in particular on the stiffness, which is the objective function subjecting the maximization.

This paper considers in theoretical and experimental analysis the of two variables, i.e. the supply pressure p_s and rotational speed n on the stiffness of axial-radial, cylindrical-frontal hydrostatic bearing. Theoretical dependencies were experimentally verified with the application of grinding spindle system of cut in center cylindrical grinder, which was equipped in a front node with analyzed axial-radial bearing.

2. Object of analysis

The design and the main characteristic dimensions of the analysed hydrostatic axial-radial bearing are shown in Fig. 1 while the numeric values are summarized in Tab. 1.

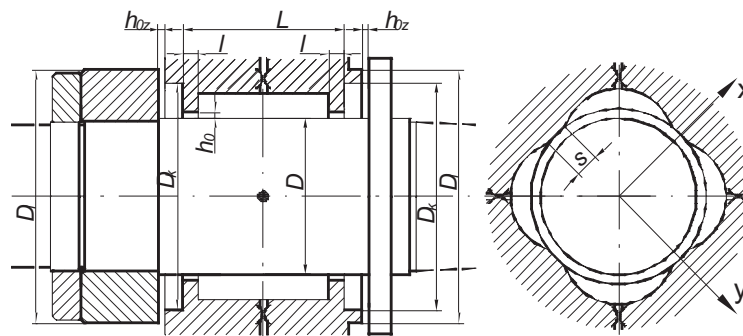


Figure 1 Principal dimensions of the hydrostatic bearings

Table 1 Characteristic dimensions of the bearing

	Magnitude	Value
Radial bearing	Diameter D [mm]	90
	Length L [mm]	134
	Radial gap h_0 [μm]	54
	Land width:	
	- leakage flow l [mm]	4
	- inter-recess s [mm]	12
	Number of packets k	4
Axial bearing	Collar diameter D_l [mm]	116
	Pockets diameter D_k [mm]	110
	Axial gap h_{0z} [μm]	29

Analysed bearing arrangement was fed with oil ISO 11158 - HL (L-HL 46) at constant pressure p_s , which was adjustable by overflow valve. Before each of pockets of radial bearing it was placed a slot restrictor with a slot face providing a laminar flow of [14], whose design with characteristic dimensions are shown in Fig. 2.

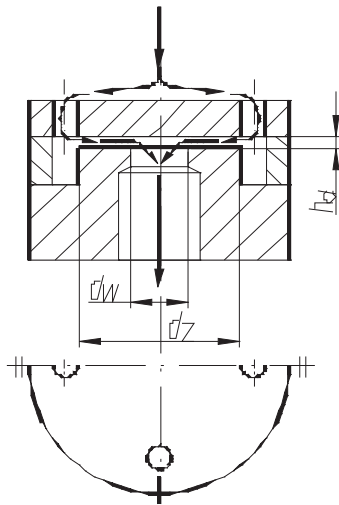


Figure 2 Principal dimensions of the hydrostatic bearings

3. Static stiffness of the bearing

Static stiffness is determined by the ratio of the increase in the applied external load to the displacement caused as a result of load actions. Loading force should be applied in such a way that its point of application and the force direction was consistent with the actual layout at the grinding [15].

Due to the fact that the verification investigation are performed using the spindle system of the grinding wheel of claw of cut in grinder, the present discussion focuses only on its radial properties. Under the terms of the cut in transverse cylindrical grinder the radial stiffness of analysed axial-radial bearing was determined for two planes Oxz (tangential force) and Oyz (thrust force).

Radial displacement of the spindle journal versus the load radial force, in accordance with [6] is described by the following equations of motion:

$$m \frac{d^2 y}{dt^2} + K_\nu \frac{dy}{dt} + K_p y + K_\omega x = W_y \quad (1)$$

$$m \frac{d^2 x}{dt^2} + K_\nu \frac{dx}{dt} + K_p x - K_\omega y = W_x \quad (2)$$

where:

- W – loading force of bearing,
- K_ν – coefficient of damping resistance [16, 17],
- K_p – pressurized component of stiffness [16, 17],
- K_ω – motional component of stiffness [16, 17].

In the case where the journal is only statically loaded then the displacement derivatives in equations (1) and (2) are equal to zero, and dependences concerning the displacement in the bearing take the following form [16]:

$$y = \frac{K_p W_y - K_\omega W_x}{K_p^2 + K_\omega^2} \quad x = \frac{K_p W_x + K_\omega W_y}{K_p^2 + K_\omega^2} \quad (3)$$

Equations (3) are accurate enough for the following assumptions and limitations:

- oil is incompressible and Newtonian fluid, and its viscosity is constant within the bearing,
- flow in the restrictors and lands of bearing is laminar,
- depth of the chamber is substantially greater than the height of slots at the steps,
- pressure drops at the lands width leakage flow and inter-recess are linear,
- relative displacements x and y are in the range [16]: $0,30 \leq x/h_0 \leq 0,30$; $-0,30 \leq y/h_0 \leq 0,30$,
- width of the lands satisfy the conditions: $0 < s \leq 0,075\pi D$; $0 < l \leq 0,15 L$.

On the basis of equation (3) the dependencies of the radial stiffness of bearing in the assumed planes Oxz and Oyz take the form [18]:

$$c_y = \frac{\Delta W_y}{\Delta y} = \frac{K_p^2 + K_\omega^2}{K_p - \frac{W_x}{W_y} K_\omega} \quad c_x = \frac{\Delta W_x}{\Delta x} = \frac{K_p^2 + K_\omega^2}{K_p + \frac{W_y}{W_x} K_\omega} \quad (4)$$

4. Experimental studies

For experimental verification of equation (4) the investigation of spindle system of grinding wheel of cut in center grinder equipped with hydrostatic bearings: front (from the grinding wheel side) and integrated axial-radial, cylindrical- face and the rear - a typical radial bearing.

Radial stiffness of the spindle system was determined for two axes Ox and Oy angularly displaced in relation to the force vector F_r . The angle between the axis Ox and the direction of the force F_r is equal to $\alpha = 45^\circ$ (Fig. 3). Therefore, it can be assumed that the spindle was loaded with two components acting along the axis Ox (tangential force) and Oy (thrust force). The values of these forces are as follows:

$$F_{rx} = F_r \cdot \sin \alpha \quad F_{ry} = F_r \cdot \cos \alpha \quad (5)$$

Lay-out of a measuring system for determination of the relationship between the spindle displacement and loads in the radial direction is shown in Fig. 3.

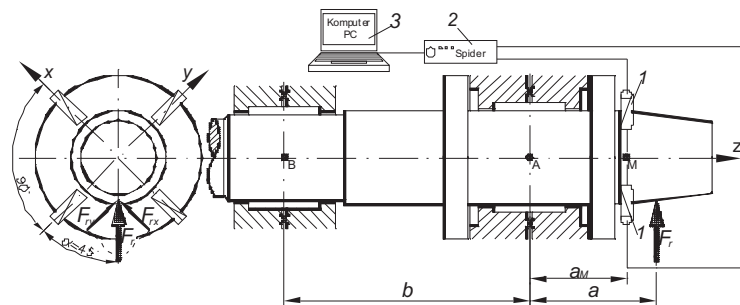


Figure 3 Lay-out of the measuring system: 1 – differential non-contact displacement measurement sensors, 2 – amplifier, 3 – computer

To determine the transverse stiffness of the axial-radial bearing the model was assumed in which the external radial force F_r is applied to the tip of the spindle at a distance $a = 170$ mm from its centre, while the non-contact sensors 1 are located at the distance equal to $a_M = 125$ mm. Displacements in the radial direction generated by force F_r were measured in two mutually perpendicular planes, Oyz and Oxz . The measurement system consists of two sets of differential non-contact displacement sensors 1, wherein the signal amplified by the amplifier 2 Spider was recorded on a PC 3 with a resolution of $0,01\mu\text{m}$. The value of the applied force is determined by a set consisting of a strain gauge force sensor (measuring range of 0 to 5 kN, accuracy class 0.05%) and the microprocessor meter (non-linearity of $< 0.0015\%$).

The displacement of the spindle in the plane Oyz caused by the force of F_{ry} are shown in Fig. 4. In the following part of this paper due to the analogy of load and displacements the detailed analysis was carried-out only the stiffness in the plane Oyz . The dependences given for the plane Oyz also apply in the plane Oxz after

the appropriate modification of recording, e.g. W_{Ax} , W_{Bx} , F_{rx} , x , c_x instead W_{Ay} , W_{By} , F_{ry} , y , c_y , and so on.

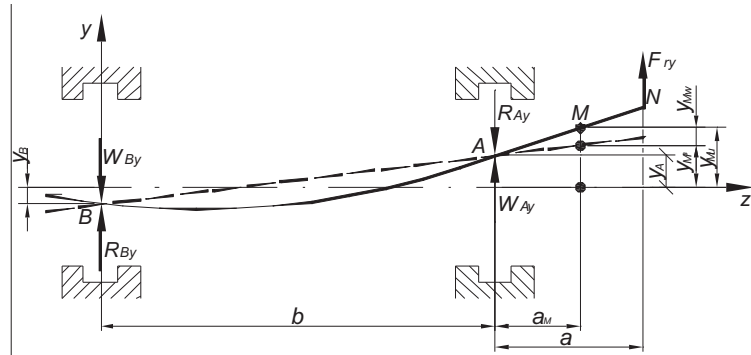


Figure 4 The displacements of the spindle in the plane Oyz caused by force F_{ry}

According to Fig. 4, as the result of the experimental investigation it was obtained a total displacement of the spindle tip at the measuring point (point M), and it is equal in the plane of action of force F_{ry} to the sum of displacements resulting from the flexibility of the bearings and the spindle:

$$y_{Mu} = y_{Ml} + y_{Mw} \quad (6)$$

where: y_{Mw} – displacement of a point M due to the flexibility of the spindle equal to [6]:

$$y_{Mw} = \lambda_M F_{ry}$$

y_{Ml} – displacement of a point M due to the flexibility of the bearings is determined from the relationship:

$$y_{Ml} = y_A \left(1 + \frac{a_M}{b}\right) - y_B \frac{a_M}{b} \quad (7)$$

Factor λ_M formulates the displacement of the point M of spindle which is supported on a perfectly rigid supports and which is caused by concentrated force, applied to a point determined by the coordinate a . Coefficient λ_M ratio is an indicator of the flexibility of the spindle in place of the sensors mounting. Considering the actual dimensions of the test spindle the value λ_M was determined by means of analytical method. For the considered system it was obtained: $\lambda_M = 5,85 \cdot 10^{-9}$ m/N.

Knowing y_{Ml} calculated from the formula (6) the searched (unknown) journal displacement in the front radial bearing the forward movement of the pivot journal bearing is y_A :

$$y_A = \frac{y_{Ml} + y_B \frac{a_M}{b}}{1 + \frac{a_M}{b}} \quad (8)$$

wherein the value y_B is considered as a known and determined by the set of theoretical dependences (3). Thus, the dependence on the radial stiffness of the axial–radial bearing obtained by experimental way is:

$$c_{Ad} = \frac{W_A}{y_A} = \frac{W_A \left(1 + \frac{a_M}{b}\right)}{y_{Ml} + y_B \frac{a_M}{b}} \quad (9)$$

Experimental study of the spindle unit was carried out for three rotational speeds n : 0, 1000, 1500 rpm and three pressures p_s values: 1.0, 1.5 and 2.0 MPa. During the investigations the viscosity of the oil flowing through the bearing was 0,0263 Pa·s.

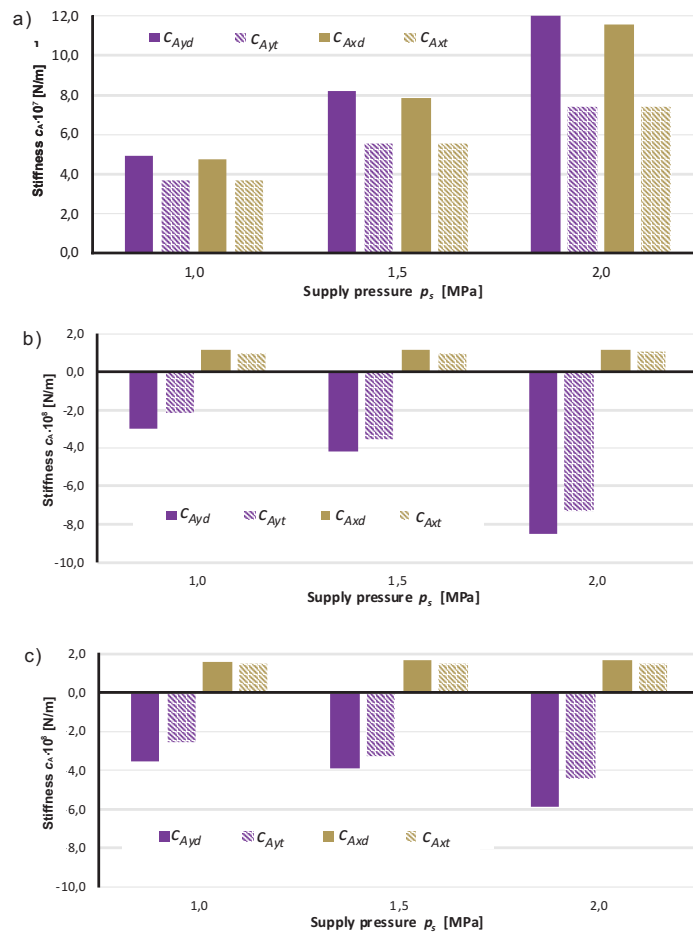


Figure 5 Radial stiffness of the axial–radial cylindrical–frontal bearing for: a) $n = 0$ rpm, b) $n = 1000$ rpm, c) $n = 1500$ rpm

In order to determine the radial stiffness of the axial–radial bearing the system was loaded by radial force F_r equal 200, 400 and 600 N. The determined characteristics

of the transverse stiffness of the axial-radial bearing hydrostatic bearing are shown in Fig. 5 in the form of bar graphs. The results concerning the experimental investigation were denoted by full fill and the results obtained by theoretical way by pattern of diagonal stripes. It should be noted that in the case of Fig. 5a it was applied the multiplier, which is less than an order than for Figs. 5b and 5c.

On the basis of the results of theoretical analysis and experimental tests it can be concluded that for a stationary spindle the stiffness is linear as a function of the supply pressure (Fig. 5a). This is confirmed by correlation coefficients R^2 fit regression line that for all obtained characteristics were not less than 0.995.

If the spindle rotates then the significant effect on its stiffness have the hydrodynamic phenomena in the bearings, which are included in the theoretical stiffness of the motion component of stiffness K_ω .

To assess the compatibility of the results obtained experimentally with the results of theoretical calculations the relative differences δ_{cx} and δ_{cy} stiffness were determined:

$$\delta_c = \frac{c_d - c_t}{c_t} \cdot 100\% \quad (10)$$

For axes Oy the most cases was characterized by the relative difference maximum of up to 20%, the largest difference was for the supply pressure of 1.0 MPa and rotational speed of 1,500 rpm and it was 40%. However, it should be noted that such a large, relative difference effects at the load, e.g. 200 N in the difference of displacement not greater than 1.0 μm . But for the axis Ox almost all test cases are characterized by maximum relative difference of 15%, only for the supply pressure of 2.0 MPa and for a stationary spindle the relative difference was larger and amounted to 29%, which resulted in a maximum difference for a load to 200 N and is equal to 0.5 μm .

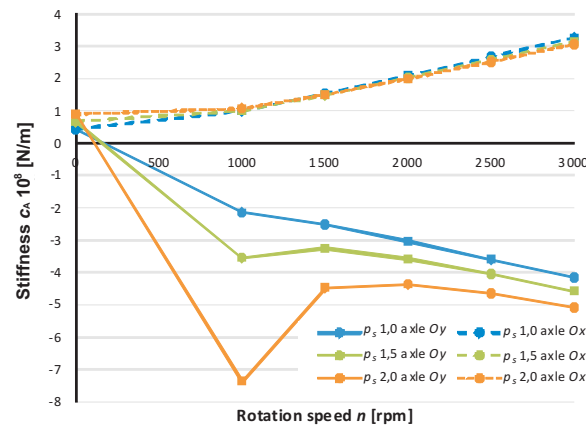


Figure 6 Dependence of the stiffness of the axial-radial bearing on the rotational speed for different supply pressure

Fig. 6 shows the characteristics of the effect of rotational speed on the stiffness of the different supply pressures in the extended speed range with respect to experimental research.

Fig. 5b, Fig. 5c and Fig. 6 show the influence of the supply pressure p_s and the rotational motion on the radial stiffness of the bearing. Attention is drawn to a much greater effect of rotational motion on the stiffness in direction of axis Oy than the axis Ox .

Particular emphasis is given the fact that in the case of the spindle rotating at 1000 rpm for a pressure of 2.0 MPa significantly higher stiffness was obtained in the direction Oy than for 1500 rpm. This situation is due to the correlation of the hydrodynamic and flow phenomena occurring between the chambers of bearing having a direct effect on the angle between the displacement and load vector [16].

It should also be noted that the studied spindle system also has significantly higher stiffness in Oyz than in Oxz plane. This feature is extremely beneficial because it is a plane of the action of grinding thrust force, and thus is decisive for the accuracy of the machine.

5. Conclusions

The results obtained according to the experimental investigation have confirmed the theoretical study that for the stationary spindle the variation in the stiffness is a linear function of supply pressure. Supply pressure directly affects the stiffness of the spindle system, which increases with pressure. In both investigated radial planes the system showed a similar stiffness.

In the case of the rotating spindle due to the hydrodynamic phenomena the radial stiffness of the hydrostatic bearings depends on the supply pressure and the rotational speed of the spindle. This speed has a clear effect on the value and direction of displacement. Rotational motion of spindle results in having several times the increase in the system stiffness of the axis Oy (reaction), which is particularly required in high-precision spindle grinding systems. Underestimation of such effect may lead to errors in the design of spindle systems with hydrostatic bearings.

It should be noted that such a significant variation in effect of rotational speed and the supply pressure on the stiffness in the direction of axis Oy may contribute, especially in the case of precision machine tools, the difficulty in obtaining the required, reproducible preciseness of parts which are machined in the case of the failure of constant parameters, i.e. the supply pressure and rotational speed.

References

- [1] Hale, L. C., Wulff, T. A. and Sedgewick, J. C.: Testing a low-influence spindle motor, *Precision Engineering*, 29, 1–10, **2005**.
- [2] Frank, W., Neugebauer, R. and Voll, H.: Nutzung des Leistungsmögens von Spindellagerungen, *Konstruktion*, 3, 53–58, **1995**.
- [3] Kane N. R., Sihler J. and Slocum A. H.: A hydrostatic rotary bearing with angled surface self-compensation, *Precision Engineering*, 27, 125–139, **2003**.
- [4] Wardle, F.: Ultra-precision Bearings, *Woodhead Publishing*, **2015**.
- [5] Zhou, L., Tachibana, T. Syoji, K., Kuriyagawa, T., Haga, T., Unno, K. and Ohshita, H.: Form mirror grinding of inner race of ceramic bearing, *Transaction of*

- the Japan Society of Mechanical Engineers*, Part C Vol. 63 No. 612 (August), 2905–2910, **1997**.
- [6] **Przybył, R.**: Podstawowe problemy projektowania zespołów wrzecionowych wyposażonych w łożyska hydrostatyczne, II. 13, 115–122, Dąbrowski L. (ed.): Obróbka ścierna w technikach wytwarzania. Badania i aplikacje. Warszawa: *Oficina Wydawnicza Politechniki Warszawskiej*, **2005**.
- [7] **Rowe, W.B.**: Hydrostatic and Hybrid Bearing Design, London, Butterworths, **1983**.
- [8] **Rowe, W. B. and O'Donoghue, J. P.**: Design Procedures for Hydrostatic Bearings, Brighton: Machinery Publishing Co. Ltd., **1971**.
- [9] **Stansfield, F. M.**: Hydrostatic bearings for machine tools, Brighton: Machinery Publishing Co. Ltd. **1970**.
- [10] **van Beek, A.**: Advanced engineering design, Delft: University of Technology, **2006**.
- [11] **Shigley, J. E., Mischke, C. R. and Brown, T. H. Jr.**: Standard Handbook of Machine Design, New York: *McGraw Hill*, **2004**.
- [12] **ISO 12168–1**, Plain bearings - Hydrostatic plain journal bearings without drainage grooves under steady-state conditions, Part 1: Calculation of oil-lubricated plain journal bearings without drainage grooves, **2001**.
- [13] **ISO 12168–2**, Plain bearings – Hydrostatic plain journal bearings without drainage grooves under steady-state conditions, Part 2: Characteristic values for the calculation of oil-lubricated plain journal bearings without drainage grooves, **2001**.
- [14] **Sikora, M.**: Metody wyznaczania charakterystyk przepływowych dławików hydraulicznych, *Mechanik*, nr 8/9, 349-354/958, **2014**.
- [15] **Kwapisz, L. and Rafałowicz, J.**: Szlifierki. WNT Warszawa, **1976**.
- [16] **Przybył, R.**: Poprzeczne łożyska hydrostatyczne w zespołach wrzecionowych obrabiarek, *Zeszyty Naukowe Politechniki Łódzkiej*, nr 921, *Wydawnictwo Politechniki Łódzkiej*, Łódź **2003**.
- [17] **Sikora, M.**: Właściwości poprzeczno-wzdłużnego łożyska hydrostatycznego, *Tribologia teoria i praktyka*, nr 2, 69–82, **2012**.
- [18] **Lewandowski, D. and Przybył, R.**: Szywność zespołu wrzecionowego łożyskowanego hydrostatycznie, *Mechanik*, 5, 273–277, **1985**.